Nonlinear Quantization for Power-Domain Non-Orthogonal Multiple Access Passive Optical Network

Kosuke Suzuoki, Daisuke Hisano, *Member, IEEE*, Sho Shibita, *Member, IEEE*, Kazuki Maruta, *Member, IEEE*, and Akihiro Maruta, *Member, IEEE*

***Abstract*—A passive optical network (PON) system is required to accommodate multi-services represented by fifth/sixth (5G/6G) mobile communication systems. While maintaining low cost, to meet these requirements (which are high capacity, low latency, and high reliability), the PON system must accommodate a large number of optical network units (ONUs). The use of power-domain non-orthogonal multiple access (PD-NOMA) for PON has been studied to increase the number of accommodatable ONUs. However, with an increase in the ratio of transmitted power between multiplexed ONUs, the effect of quantization noise in the analog-to-digital converter (ADC) is more significant. This study proposes to apply an optimal quantizer based on the Lloyd-Max algorithm (which is a nonlinear quantization algorithm) to PD-NOMA-PON. In general, the Lloyd-Max algorithm requires continuous probability density function when setting the partitions. We adopt a continuous function estimated from the discrete probability distribution extracted by the low-resolution ADC using an expectation maximization algorithm. We conduct experiments to verify the feasibility of the proposed quantizer for the downlink and confirm the improvement of the optical signal-to-noise ratio penalty for all power ratios.**

***Index Terms*—Quantization (signal), noise reduction, optical network units, optical fiber communication, passive optical networks, optical noise, signal to noise ratio.**

I. Introduction

FUTURE optical access networks should support continuously growing requirements for mobile communication services such as extremely high capacity and ultra-low latency. Passive optical network (PON) systems with a digital coherent scheme [1] and wavelength division multiplexing (WDM) are key technologies to cover the abovementioned service trends [2], [3]. The digital signal processing (DSP)-enabled PON system promises expanding the link budget and improving the transmission capacity. For low-latency transmission, an optical line terminal (OLT) at an operator side with the WDM system allocates different wavelengths to each optical network unit (ONU) at a subscriber side to lay out each independent optical path. Meanwhile, it is difficult to cost-effectively accommodate the number of ONUs in a single PON system limited by the available bandwidth and economic considerations. For these reasons, not only a point-to-point WDM overlay scheme but also a hybrid configuration of a time-division multiplexing (TDM) scheme and WDM scheme, termed TWDM, has been standardized in ITU-T G.989.2 [4]. TWDM scheme continues to meet the demands for expanding the capacity. Meanwhile, in recent years, optical access network systems are being exposed the more advanced requirements. The TDM scheme has a waiting time for transmission caused by sharing a time slot among all users using the same wavelength, which increases the transmission delay. In contrast, the use of non-orthogonal multiplexing techniques, termed power-domain non-orthogonal multiple access (PD-NOMA) scheme, has been recently studied in the wireless communication field [5]. In these years, employing NOMA on visible light communication systems has been widely considered [6]. As the example of the optical fiber communication field, a hierarchical modulation (HM) scheme, similar to the NOMA scheme, has already been proposed for the downlink transmission [7]. Fig. 1 shows an overview of the NOMA techniques. The PD-NOMA-PON system conducts non-orthogonal multiplexing of optical signals in the power

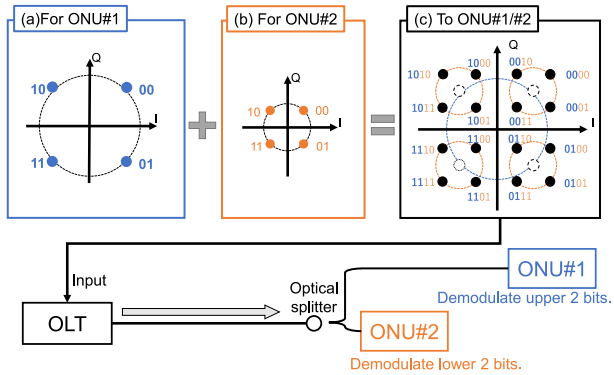

Fig. 1. Overview of PD-NOMA-PON system.

Manuscript received March 24, 2021; revised June 6, 2021; accepted July 5, 2021. Date of publication July 8, 2021; date of current version October 4, 2021. This work was supported in part by the Telecommunications Advancement Foundation, Japan, and in part by JSPS KAKENHI under Grant JP20H04178. *(Corresponding author: Daisuke Hisano.)*

Kosuke Suzuoki, Daisuke Hisano, Sho Shibita, and Akihiro Maruta are with the Graduate School of Engineering, Osaka University, Suita 565-0871, Japan (e-mail: suzuoki@pn.comm.eng.osaka-u.ac.jp; hisano@comm.eng.osaka-u.ac.jp; shibita@pn.comm.eng.osaka-u.ac.jp; maruta@comm.eng.osaka-u.ac.jp).

Kazuki Maruta is with the Academy for Super Smart Society, Tokyo Institute of Technology,, Tokyo 152-8550, Japan (e-mail: kazuki.maruta@ieee.org).

Color versions of one or more figures in this article are available at https://doi.org/10.1109/JLT.2021.3095567.

Digital Object Identifier 10.1109/JLT.2021.3095567

domain. Introducing the non-orthogonal multiplexing scheme into the conventional orthogonal ones, e.g., WDM or TDM, the number of ONUs to be accommodated can be increased while reducing the transmission delay.

In the PD-NOMA system, the power ratio of the multiplexed optical signals transmitted to each ONU depends on the link budget of the optical link. However, as the power ratio allocated to each ONU is larger, the Euclidean distance on the IQ plane of the power-multiplexed signal is smaller. Thus, the quantization noise in the analog-to-digital converter (ADC) of the OLT or ONU degrades the signal-to-noise (SNR) power ratio. To reduce the quantization noise, this paper proposes to apply the Lloyd-Max quantization (LMQ) algorithm [8] for PD-NOMA-PON. We conduct experiments and evaluate the system performance of LMQ. The measurement result of optical SNR (OSNR) elucidates the reduction of the penalty. This study extends the analytical results from the previous work presented at the European Conference on Optical Communication (ECOC)2020 [9].

II. PD-NOMA-PON System

This section presents the fundamentals of the PD-NOMA scheme. In this study, we assume a downlink transmission from the OLT to the ONU. First, the OLT extracts a pair of ONUs in the same PON branch and assigns a different power to each ONU at the same center frequency. A wireless system adaptively changes the combination of terminals depending on the channel status. Meanwhile, the channel in the PON link is stable compared with the wireless channel. Thus, the trigger of changing a pair of ONUs is the request of the bandwidth, not the channel state. Fig. 1(a) and (b) show the constellation map of each ONU when employing a QPSK scheme. In the PD-NOMA scheme, these two signals with different power are linearly superimposed, as shown in Fig. 1(c). The multiplexed signal in this scheme is expressed by the following equation:

$$s = \sqrt{P_1}s_1 + \sqrt{P_2}s_2 \tag{1}$$

Here, P_1 and P_2 ($P_1 > P_2$) represent the average power of the signals of each ONU. Based on this relationship, the power ratio is defined as P_1/P_2. The power ratio P_1/P_2 is determined at the OLT side by the difference in the link budget between the ONUs. If the power ratio is more extensive, P_1 increases and P_2 decreases because the transmission power is constant. As a result, the link budget of ONU#1 increases and the link budget of ONU#2 decreases. From the relationship between the link budget and the power ratio described above, the OLT must select a suitable power ratio according to the desired link budget to enable both ONUs to communicate.

Here, we describe the demodulation method. When ONU#1 in Fig. 1 demodulates the own signal, the signal of ONU#2 is regarded as the noise component. Thus, ONU#1 regards the multiplexed signal as the simple QPSK signal. On the other hand, when ONU#2 demodulates its own signal, there are two typical demodulation methods. The first method is to equalize and demodulate the multiplexed signal in a QAM format. The signal is separated according to the bit assignment of each symbol. For example, in Fig. 1(c), the bits assigned to ONU#2 are the lower 2 bits in 4 bits. Therefore, only the lower 2 bits out of 4 bits obtained by determining 16 types of symbols are received. This demodulation method is also known as the HM method [7]. Another method is to perform successive interference cancellation with forwarding error correction (FEC) [10]. In this paper, we used the HM method, but our proposed nonlinear quantizer can be applied to both methods. Therefore, in this paper, we do not mention the superiority and inferiority of the methods.

PD-NOMA-PON systems have a challenging issue, that is, quantization noise. A low-resolution ADC is installed in high-speed coherent PON systems from the viewpoints of power consumption and implementation cost. Fig. 2 shows the effect of quantization noise when the power ratio increases. A linear quantizer, which is typical in an optical communication system, produces quantization noise. Quantization noise is directly proportional to the available amplitude and the quantization width. The quantization width is determined from the number of quantization. An ADC at the receiver samples and quantizes the PD-NOMA signal. The quantizer produces a uniform quantization noise that is independent of the power ratio between the signals from the ONUs. When the power ratio is larger, the quantization noise cannot be ignored for the signal with smaller power.

III. LMQ Based Receiver

This section describes LMQ as a nonlinear equalizer in ADCs and digital-to-analog converters (DACs). The downlink PD-NOMA system multiplexes the signals in the digital domain. When the power ratio is large, a DAC in the transmitter and an ADC in the receiver do not fully utilize their dynamic range for the signal with a smaller power allocation. While the PD-NOMA scheme changes the power ratio, the quantization noise greatly affects the signal quality because the power ratio is larger. We aim to reduce the quantization noise and employ LMQ in the PD-NOMA system.

A. Variable Definition

LMQ searches for a partition and a rounding value, which are quantization parameters. Using this approach, the mean square of the quantization noise is minimized with respect to the amplitude distribution of the multiplexed signal. LMQ conducts the iterative calculation and properly converges the partition and the rounding value. Let $\{m = 1, 2, \ldots, M \in N_+\}$ denote the iteration numbers. When the iteration number reaches M times, the iterative calculation of LMQ is halted and obtains the optimal parameters. Let N and $p(x)$ be the number of quantization bits and the probability density function (PDF) of the amplitude distribution of the multiplexed signal, respectively. Let $x_\nu^{(m)}(\nu = 1, 2, \ldots, 2^N - 1 \in N_+)$ and $q_\alpha^{(m)}(\alpha = 1, 2, \ldots, 2^N \in N_+)$ denote the quantization partition and quantization rounding value for the m–th iteration, respectively. Fig. 3 shows the relationship between $x_\nu^{(m)}$, $q_\alpha^{(m)}$ and $p(x)$.

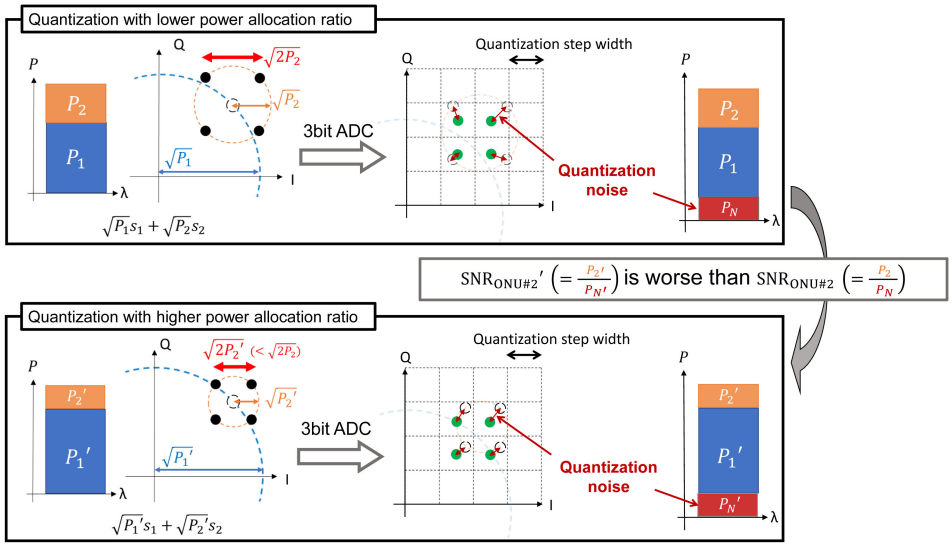

Fig. 2. Influence of quantization noise in PD-NOMA-PON system.

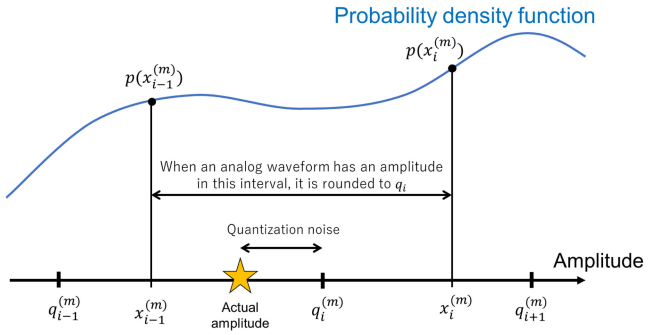

Fig. 3. Relationship of $x_\nu^{(m)}$, $q_\alpha^{(m)}$ and $p(x)$.

B. LMQ Algorithm

For a given quantization parameter, the mean square error (MSE) of the quantization noise e is given by

$$E[e^2] = \sum_{i=1}^{2^N} \int_{x_{i-1}}^{x_i} (x - q_i)^2 p(x) dx, x_0 = -\infty, x_{2^N} = \infty, \tag{2}$$

where the set number is omitted for simplicity. Note that $E[\cdot]$ means the average value. Differentiate $E[e^2]$ with respect to x_i and q_i, and the minimum $E[e^2]$ is obtained when both are zero. This is expressed as

$$\frac{dE[e^2]}{dx_i} = 0, \frac{dE[e^2]}{dq_i} = 0. \tag{3}$$

LMQ solves Eq. (3) according to the following update algorithm. Fig. 4 shows a schematic diagram of LMQ. LMQ alternately updates the partition x_ν and the rounding value q_α. When $m = 1$, we apply the quantization parameters of a linear quantization as an initial state. To obtain the $(m+1)$-th set, the rounding value $q_\alpha^{(m+1)}$ is updated by

$$q_1^{(m+1)} = \frac{\int_{-\infty}^{x_1^{(m)}} xp(x)dx}{\int_{-\infty}^{x_1^{(m)}} p(x)dx}, \tag{4}$$

$$q_i^{(m+1)} = \frac{\int_{x_{i-1}^{(m)}}^{x_i^{(m)}} xp(x)dx}{\int_{x_{i-1}^{(m)}}^{x_i^{(m)}} p(x)dx}, \tag{5}$$

$$q_{2^N}^{(m+1)} = \frac{\int_{x_{2^N-1}^{(m)}}^{\infty} xp(x)dx}{\int_{x_{2^N-1}^{(m)}}^{\infty} p(x)dx}, \tag{6}$$

where $i = \{2, 3, \ldots, 2^N - 1 \in N_+\}$. Note that the integral of the numerator is not always obtained analytically. However, in this case, it can be obtained analytically because $p(x)$ is a Gaussian mixture distribution. The details are described in the next section. The partition $x_\nu^{(m)}$ in the $m+1$-th iteration is updated by

$$x_\nu^{(m+1)} = \frac{1}{2}\left(q_\nu^{(m+1)} + q_{\nu+1}^{(m+1)}\right). \tag{7}$$

LMQ sufficiently repeats this procedure. The partition and rounding value that minimize the MSE of the quantization noise can be obtained.

C. Estimation of the PDF of the Amplitude Distribution

LMQ requires the PDF, which is a continuous function when setting the partitions. Strictly speaking, the sufficient-resolution ADC is required, but it is difficult to install the high-resolution ADC in an ONU. Therefore, we adopt the function that estimates the continuous distribution from the discrete probability distribution extracted by the low-resolution ADC using the expectation maximization (EM) algorithm [11]. The EM algorithm fits a Gaussian mixture model (GMM) to the estimated distribution. Noise in the propagation path basically behaves as an additive white Gaussian noise. Thus, the amplitude distribution

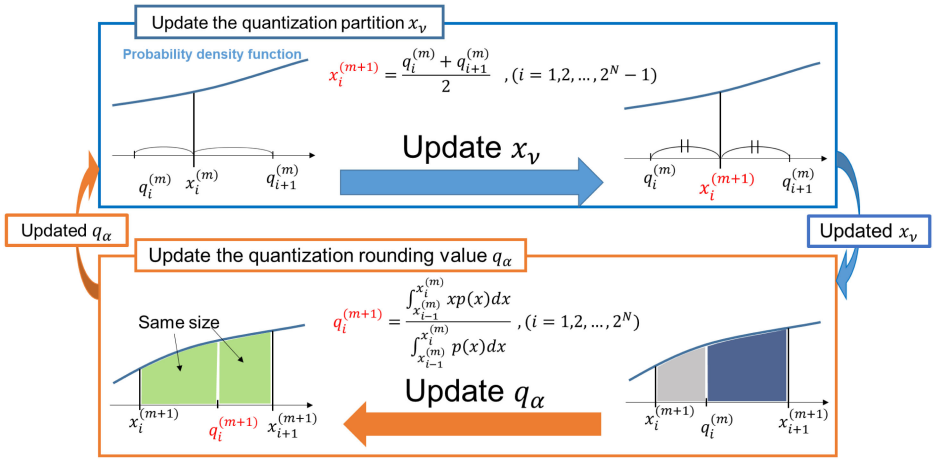

Fig. 4. Lloyd–Max algorithm.

of the signal is a superposition of several Gaussian distributions. Therefore, fitting by the GMM is sufficient to obtain superior performance.

D. Contribution

The PD-NOMA system has been widely studied in the wireless communication system field to improve the spectral efficiency in a limited available bandwidth [12]. Employing the NOMA scheme in the 5th mobile communication system (5G) has been considered [13]. The difference between wireless and optical access systems is that the optical access system has a more stable channel. Meanwhile, the number of quantization bits in an ADC is small. Owing to the stationarity of the optical channel, which is an advantage of optical access networks, the scale of the received amplitude does not change rapidly. In addition, assuming coherent reception, the phase can be regarded as random owing to the carrier frequency offset (CFO); thus, the received amplitude is the same for the I-channel and Q-channel, and the effect of time-varying phase noise on the distribution can be ignored. Therefore, the ONU does not need to frequently update the quantization parameters. Under these constraints, LMQ has a tremendous contribution to the PD-NOMA-PON system.

In addition, the proposed technique applies to other reception schemes, e.g., intensity modulation direct detection (IMDD)-based modulation signals. This is because the proposed scheme is employed on the ADC/DAC. Note that the effectiveness of the technique depends on the amplitude distribution of the modulated signal. In particular, it can be helpful in orthogonal frequency division multiplexing (OFDM) and discrete multi-tone (DMT) modulated signals since having the Gaussian-like amplitude distribution.

IV. Experiments

A. Setup

We experimentally evaluated the feasibility of the proposed LMQ technique employed in the PD-NOMA-PON system. Fig. 5(b) shows the experimental setup. This setup aims to measure the bit error rate (BER) by changing the OSNR. Fig. 5(a) shows the offline process at the transmitter side to generate the PD-NOMA multiplexed signal to input into an arbitrary waveform generator (AWG).

1) Transmitter Side and Channel: We generated two QPSK signals with a pseudo-random bit sequence (PRBS) having $2^{15} - 1$ bits and linearly combined the two signals. Here, we term the combined signal as the PD-NOMA signal. To suppress the correlation between each channel data sequence, we provided a 1000-bit shift to each channel data. After generating the PD-NOMA signal, we add a pilot signal of the QPSK format to the head of the PD-NOMA signal for symbol synchronization. The PD-NOMA signal was twofold up-sampled by zero padding and filtered using a root-raised cosine (RRC) filter with a roll-off rate of 0.25. The PD-NOMA signal was input into the AWG, which generated a 20-Gbaud analog RF signal. Note that the frequency response of AWG was pre-equalized. A laser diode (LD) with a linewidth of $<$ 100 kHz was used.

2) Channel: The amplified spontaneous emission (ASE) light output from an erbium-doped fiber amplifier (EDFA) is coupled with the multiplexed signal at a 3-dB optical coupler. A variable optical attenuator (VOA) adjusted the OSNR. An optical spectrum analyzer (OSA) measured the OSNR in the frequency domain. To measure the OSNR correctly, the OSA is installed before an optical bandpass filter (OBPF). The noise level is obtained from outside of the signal bandwidth. The second VOA, inserted between the OBPF and the coherent receiver, is to fix the received power at 0 dBm. Note that the VOA does not change the OSNR.

3) Receiver Side: A coherent receiver and a local oscillator (LO) with a linewidth of $<$ 1 kHz were used to detect the optical signal. Then, a digital storage oscilloscope (DSO) sampled and quantized the RF signal with an 8-bit linear quantizer at a sampling rate of 160 GSa/s. After the quantization by DSO, a digital signal processing (DSP) unit performs demodulation to extract bit sequences for each transmitter.

4) DSP: Fig. 5(c) shows the functional blocks of the DSP. The received signal with a sampling rate of 160 GSa/s was

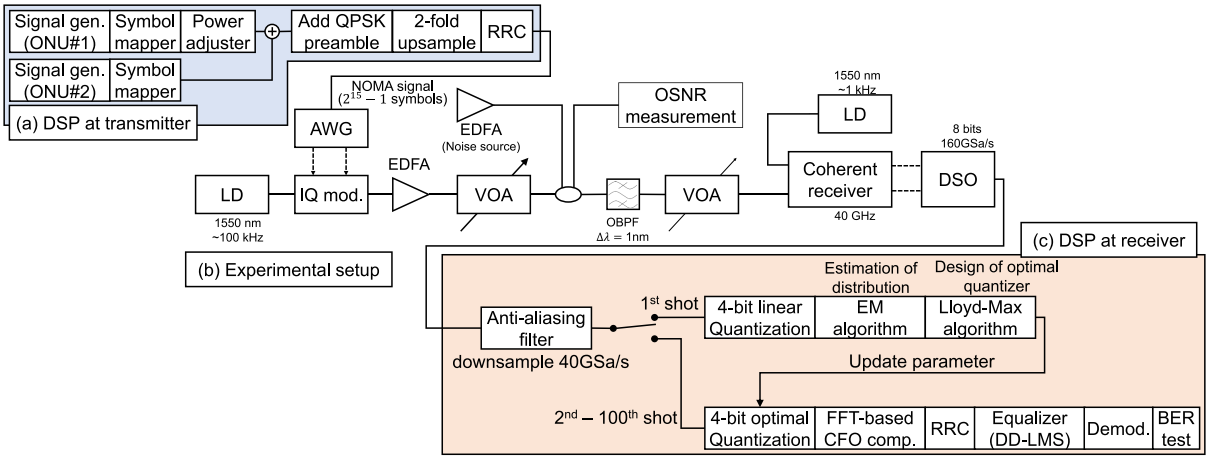

Fig. 5. Setup.

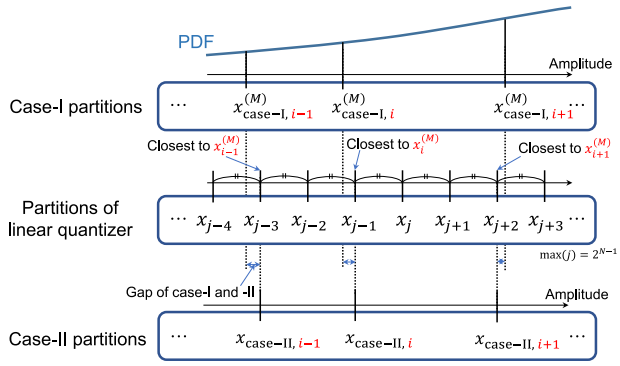

Fig. 6. The difference of partition setting between LMQ case-I and case -II.

resampled to 40 GSa/s using an anti-aliasing digital filter. We conducted the proposed LMQ to the resampled signal.

Before introducing LMQ, we discussed the two types of ADCs with the proposed LMQ.

- The first is the case where the ADC can set partitions to arbitrary value.
- The second is the case where the partitions of the ADC are fixed.

The relationship between the two types of ADC, defined as case-I and case-II partitions, is shown in Fig. 6.

LMQ with case-I : To evaluate the first case, we used a 4-bit linear quantizer and calculated the discrete distribution of the amplitude of the PD-NOMA signal. Then, the continuous distribution was estimated using the EM algorithm. Finally, we set the partitions to the arbitrary and desired position flexibly. This type of quantizer has been reported in our previous work [9], and is defined as case-I in this paper.

5) LMQ With case-II: Next, in the latter case where the partitions of the ADC are fixed, it is not easy to install the proposed LMQ in the ADC because the positions of partitions cannot be changed, even though the proposed LMQ finds the proper partitions. Meanwhile, it is useful in terms of reducing the number of bits used by a linear quantizer with a certain number of bits. The ADC quantized the PD-NOMA signal with 6 or 8 bits. Then, the discrete distribution of the amplitude was calculated. Afterward, the continuous distribution was estimated using the EM algorithm. Using a continuous distribution, LMQ calculated the ideal position of partition. However, the ADC may not have the position of partition because it cannot be moved from the initial position. Therefore, LMQ chooses a partition that is the closest calculated partition from the initial set of partitions. Note that in this paper, we term the latter case as case-II.

6) Evaluation Metric: This study compared the 4-bit linear quantizer with the 4-bit LMQ for case-I using the required OSNR in the hard-decision FEC limit (BER $= 3.8 \times 10^{-3}$ at output BER $= 10^{-13}$) [14]. Then, a 4-bit LMQ at case-II was compared with the linear quantizer using the BER. For the experimental parameters, the Lloyd-Max algorithm requires training data. We transmitted the multiplexed signals of 100 shots in sequence and used the first shot as training data. In DSP, we first coarsely compensated CFO using an FFT-based compensator [15]. Next, we applied the same RRC filter as in the transmitter side. Then, adaptive equalization was performed in the time domain. A decision-directed least mean square (DD-LMS) algorithm was used in the adaptive equalizer, with 9 taps and a step size of 4.0×10^{-4}. After adaptive equalization, the BER was measured. In the abovementioned evaluation, we used a long length of training symbols to estimate the continuous amplitude distribution. We revealed the desired number of training symbols to estimate the continuous distribution, because the shorter the length of training symbols, the higher the usage efficiency. We used the Kullback-Leibler (KL) divergence as an evaluation metric [16].

B. Experimental Results

1) 8-Bit Linear Quantization: Fig. 7 shows the BER curves of ONU#1 and ONU#2 using an 8-bit linear quantizer. Power ratios (P_1/P_2) were set to 4, 6, and 10. We used these results as a baseline. Fig. 8 (i) (ii) (iii) show a comparison of the PDF estimated by the EM algorithm assuming a GMM and the discrete distribution of the received signals quantized by the 8-bit linear quantizer. These results reveal that the received signals follows the GMM.

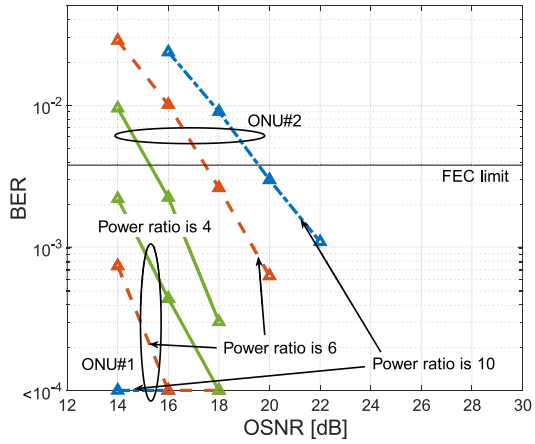

Fig. 7. BER curves for ONU#1 and ONU#2 with 8-bit linear quantizer.

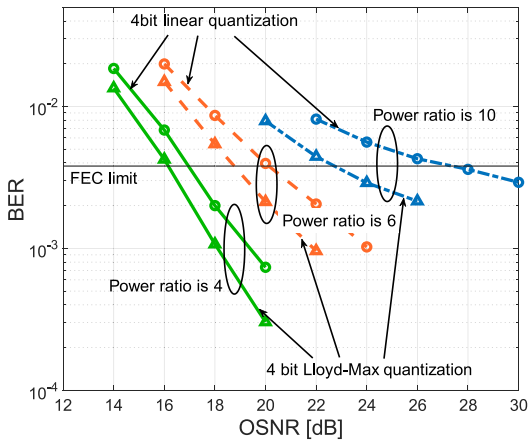

Fig. 9. BER curves for ONU#2 with linear quantizer and LMQ.

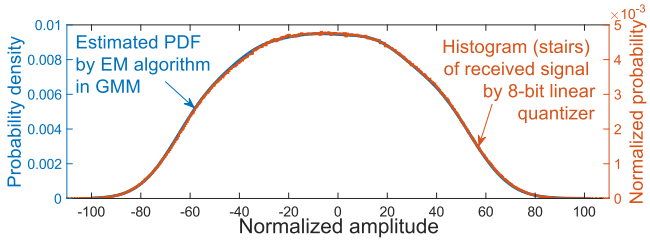

(i) The power ratio is 4 and the OSNR is 16 dB.

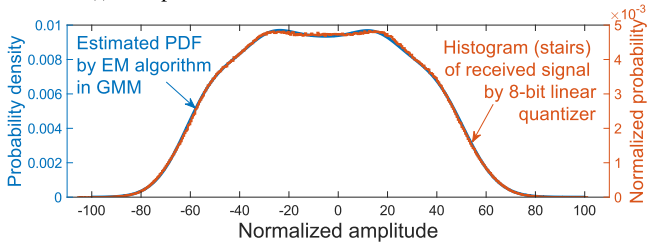

(ii) The power ratio is 6 and the OSNR is 20 dB.

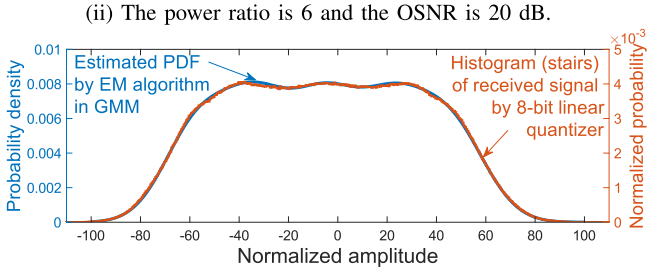

(iii) The power ratio is 10 and the OSNR is 24 dB.

Fig. 8. Comparison between the estimated distribution and the signal received by the 8-bit linear quantizer.

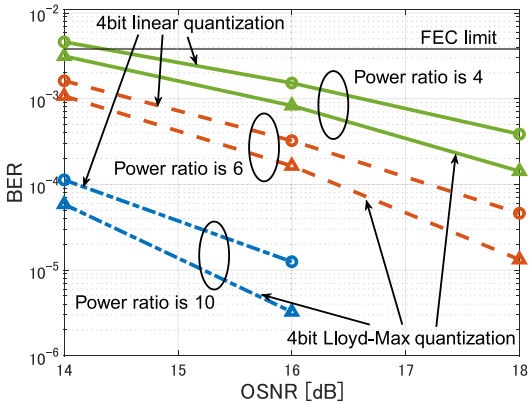

Fig. 10. BER curves for ONU#1 with linear quantizer and LMQ.

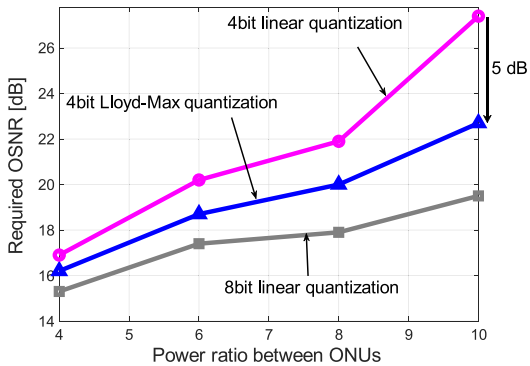

Fig. 11. Required OSNR of ONU#2 for each quantization method.

2) LMQ With Case-I: Fig. 9 shows the BER curve of ONU#2 to which a small signal power is allocated. LMQ reduced the OSNR penalty for all power ratios compared to the linear quantizer. Fig. 10 shows the BER curve of ONU#1 to which a large signal power is allocated. Although the OSNR could not be reduced below 14 dB due to the experimental setup, The OSNR penalty decreased for all power ratios. Fig. 11 shows the required OSNR to satisfy the FEC limit extracted from Fig. 9. When the power ratio was larger, the OSNR penalty was improved drastically. When the power ratio increases, the inter-symbol distance of the ONU#2 signal decreases, making it more sensitive to the quantization noise. When the power ratio was 10, the OSNR penalty can be improved by 5 dB maximally and approaches to the characteristics of 8-bit quantization. Note that we assumed the preamplifier type receiver. The received optical power was maintained constantly. In other words, the dominant noise is amplified spontaneous emission (ASE) noise generated in the preamplifier. Therefore, the link budget is directly increased by the OSNR improvement.

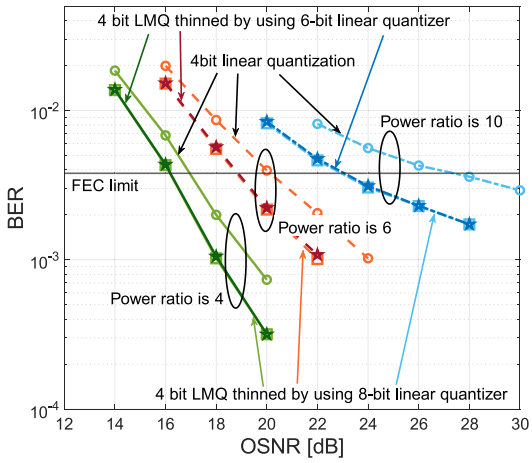

Fig. 12. BER curves for ONU#2 with 4-bit linear quantizer and 4-bit LMQ thinned by using 6-bit or 8-bit linear quantizer.

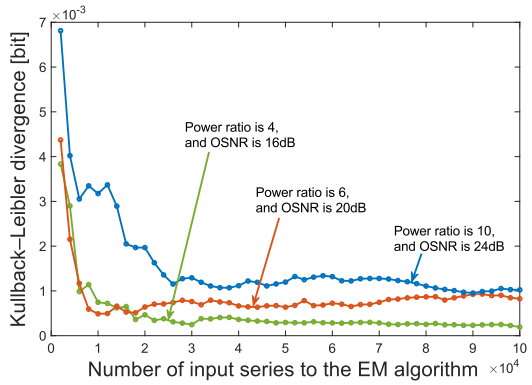

Fig. 13. Convergence of distribution estimation for number of training series by EM algorithm.

3) LMQ With case-II: Fig. 12 shows the BER curve of ONU#2 to which a small power is allocated. We calculated the ideal partitions with a 4-bit resolution based on LMQ and EM algorithms. Then, we ideally set the partitions to the closest one in 6-bit or 8-bit resolution. As a result, there was no significant difference between the 6-bit and 8-bit partitions, we obtained comparable OSNR penalties to those in Fig. 9. A 6-bit linear quantizer is sufficient to reproduce LMQ using the partition of the linear quantizer.

4) Required Training Symbol Length: The KL divergence is known as a metric to measure the difference between two distributions of random variables. Here we prepared these variables as 100-shot data and the first one from it; each of them produces distribution of p_1 and p_2, respectively. Therefore, we prepared a distribution p_1 estimated using 100-shot data. An ADC conducted a twofold oversampling for the symbol rate and quantized each IQ-channel. Thus, the distribution was generated by the training symbols of $100 \times (2^{15} - 1) \times 2 \times 2 = 13.1 \times 10^6$. Next, we changed the number of training symbols of the first shot data and estimated the continuous distribution p_2. Finally, we calculated the KL divergence between p_1 and p_2. In this case, since p_1 is considered to be close to the actual distribution, the KL divergence is calculated by $\int_{-\infty}^{\infty} p_1(x) log(p_1(x)/p_2(x)) dx$.

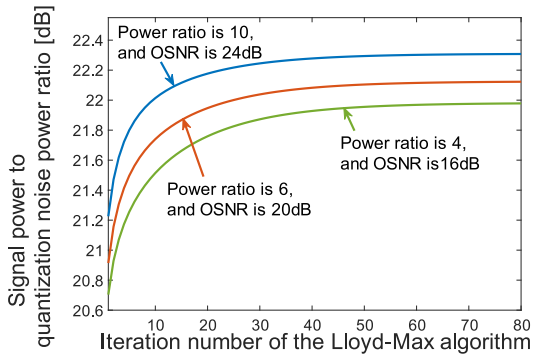

Fig. 14. Variation of the amount of quantization noise with respect to the iteration number of the Lloyd-Max algorithm.

Fig. 13 shows the result of the KL divergence. The convergence point was different depending on the power ratio and OSNR. 30 000 symbols is sufficient. LMQ requires an iterative calculation to converge partitions to correct positions. Here, we investigated the number of required iterations. Fig. 14 plots the ratio of the signal power to the quantization noise power with the iteration count, when the power ratios are 4, 6, and 10 obtained by the experiments. The signal power was obtained from the PDF estimated by the EM algorithm. The quantization noise was calculated as the quantization error calculated from the difference between the signals before and after quantization. We calculated the signal and quantization noise powers for each iteration. Approximately 80 iterations are required to converge LMQ output flatly.

V. Conclusion

This study proposed LMQ to digital coherent-based PD-NOMA-PON systems. LMQ improves the OSNR with a low-resolution ADC. We experimentally demonstrated the effectiveness LMQ for signals multiplexed by the PD-NOMA scheme at 20 Gbaud. We confirmed an improvement in the OSNR penalty at all power ratios of 4, 6, and 10. In particular, when the power ratio was 10, the OSNR penalty was reduced drastically by approximately 5 dB. Furthermore, even when the partitions of the ADC cannot be moved, we indicated that LMQ could be employed by reducing the number of used bits of the ADC. When 4-bit LMQ is required, we can obtain LMQ by thinning out the partitions from a linear quantizer with a minimum of 6 bits. Using the KL divergence as an indicator, we calculated the number of training symbols required to estimate the continuous distribution of the amplitude of signal used in LMQs. Furthermore, we indicated that the required number of iterations required to design LMQ was approximately 80. The NOMA scheme enables a coherent PON system to increase the number of ONUs without additional devices. In the NOMA-PON system, the proposed scheme can contribute to extending the link budget.

Acknowledgment

We are grateful to Keysight Technologies for lending us AWG M8194 A.

REFERENCES

[1] K. Kikuchi, "Fundamentals of coherent optical fiber communications," *J. Lightw. Technol.*, vol. 34, no. 1, pp. 157–179, 2016.

[2] N. Yoshimoto, J. Kani, S. Kim, N. Iiyama, and J. Terada, "DSP-based optical access approaches for enhancing NG-PON2 systems," *IEEE Commun. Mag.*, vol. 51, no. 3, pp. 58–64, Mar. 2013.

[3] N. Suzuki, H. Miura, K. Matsuda, R. Matsumoto, and K. Motoshima, "100 Gb/s to 1 Tb/s based coherent passive optical network technology," *J. Lightw. Technol.*, vol. 36, no. 8, pp. 1485–1491, 2018.

[4] ITU-T G.989.2, "40-Gigabit-capable passive optical networks 2 (NG-PON2): Physical media dependent (PMD) layer specification - Amendment 1," 2019.

[5] J. A. Altabas *et al.*, "Nonorthogonal multiple access and carrierless amplitude phase modulation for flexible multiuser provisioning in 5G mobile networks," *J. Lightw. Technol.*, vol. 35, no. 24, pp. 5456–5463, 2017.

[6] R. C. Kizilirmak, C. R. Rowell, and M. Uysal, "Non-orthogonal multiple access (NOMA) for indoor visible light communications," in *Proc. 4th Int. Workshop Opt. Wireless Commun.*, 2015, pp. 98–101, doi: 10.1109/IWOW.2015.7342274.

[7] N. Iiyama, J. Kani, J. Terada, and N. Yoshimoto, "Feasibility study on a scheme for coexistence of DSP-based PON and 10-Gbps/2303ı PON using hierarchical star QAM format," *J. Lightw. Technol.*, vol. 31, no. 18, pp. 3085–3092, 2013.

[8] S. Lloyd, "Least squares quantization in PCM," *IEEE Trans. Inf. Theory*, vol. 28, no. 2, pp. 129–137, Mar. 1982.

[9] K. Suzuoki, D. Hisano, S. Shibita, K. Maruta, and A. Maruta, "Experimental demonstration of Lloyd-max algorithm to quantization noise reduction on a power-domain non-orthogonal multiple access based coherent PON," in *Proc. Eur. Conf. Opt. Commun.*, Brussels, 2020, pp. 1–4, doi: 10.1109/ECOC48923.2020.9333348.

[10] F. Lu, M. Xu, L. Cheng, J. Wang, J. Zhang, and G. Chang, "Non-orthogonal multiple access with successive interference cancellation in millimeter-wave radio-overfiber systems," *J. Lightw. Technol.*, vol. 34, no. 17, pp. 4179–4186, 2016.

[11] C. M. Bishop, *Pattern Recognition and Machine Learning*. New York: Springer, 2006.

[12] K. Higuchi and A. Benjebbour, "Non-orthogonal multiple access (NOMA) with successive interference cancellation for future radio access," *IEICE Trans. Commun.*, vol. E 98-B, no. 3, pp. 403–414, 2015.

[13] NTT docomo, "DOCOMO 5G White Paper," [Online]. Available: https://www.nttdocomo.co.jp/english/binary/pdf/corporate/technology/whitepaper_5 g/DOCOMO_5G_White_Paper.pdf, Retrieved on Jul. 15, 2021.

[14] ITU-T G.975.1, "Forward error correction for high bit-rate DWDM submarine systems Corrigendum 2," Jul. 2013..

[15] T. Nakagawa *et al.*, "Non-data-aided wide-range frequency offset estimator for qam optical coherent receivers," in *Proc. Opt. Fiber Commun. Conf. Expo. Nat. Fiber Opt. Eng. Conf.*, 2011, pp. 1–3.

[16] S. Kullback and R.A.Leibler. "On information and sufficiency," *Ann. Math. Statist.*, vol. 22, no. 1, 79–86, 1951.

Kosuke Suzuoki received the B.E. degree in electrical, electronic and information engineering from Osaka University, Osaka, Japan, in 2020. He is currently working toward the M.E. degree with the Graduate School of Engineering, Osaka University. His research interests include power-domain non-orthogonal multiple access and optical fiber communication. He is a Student Member of the Institute of Electronics, Information, and Communication Engineers of Japan.

Daisuke Hisano (Member, IEEE) received the B.E, M.E, and Ph.D. degrees in electrical, electronic and information engineering from Osaka University, Osaka, Japan, in 2012, 2014, and 2018, respectively. In 2014, he joined NTT Access Network Service Systems Laboratories, Yokosuka, Japan. Since October 2018, he has been an Assistant Professor with Osaka University. His research interests include optical-wireless converged networks, optical communication, all-optical signal processing, visible light communication, edge computing, and application of deep learning to optical communication. He is a Member of the IEICE.

Sho Shibita (Member, IEEE) received the B.E. and M.E. degrees in electrical, electronic and information engineering from Osaka University, Osaka, Japan, in 2018 and 2020, respectively. He is currently working toward the D.E. degree with the Graduate School of Engineering, Osaka University. His research interests include single-wavelength bidirectional transmission and optical fiber communication. He is a Student Member of the Institute of Electronics, Information, and Communication Engineers of Japan.

Kazuki Maruta (Member, IEEE) received the B.E., M.E., and Ph.D. degrees in engineering from Kyushu University, Fukuoka, Japan, in 2006, 2008, and 2016, respectively. From 2008 to 2017, he was with NTT Access Network Service Systems Laboratories. From 2017 to 2020, he was an Assistant Professor with the Graduate School of Engineering, Chiba University, Chiba, Japan. He is currently a Specially Appointed Associate Professor with the Academy for Super Smart Society, Tokyo Institute of Technology, Tokyo, Japan. His research interests include MIMO, adaptive array signal processing, channel estimation, medium access control protocols, and moving networks. He is also a Member of the Institute of Electronics, Information and Communication Engineers (IEICE). He was the recipient of the APMC2014 Prize and the IEEE ICCE2021 Excellent Paper Award. He was the co-recipient of the IEICE Best Paper Award in 2018, the SoftCOM2018 Best Paper Award, and the APCC2019 Best Paper Award.

Akihiro Maruta (Member, IEEE) received the B.E., M.E., and Ph.D. degrees in communications engineering from Osaka University, Osaka, Japan, in 1988, 1990, and 1993, respectively. In 1993, he was with the Department of Communications Engineering, Osaka University. Since 2016, he has been a Professor with the Department of Information and Communication Technology, Osaka University. His current research interests include optical fiber communication systems and all-optical signal processing. He is a Member of the IEEE Photonics Society and the Optical Society of America.